International Journal of Thermophysics, Vol. 13, No. 1, 1992

Aspects of High-Temperature Pyrometry for Measurements in Ultrahigh Vacuum[1]

P. Neuhaus,[2] I. Egry,[2] and G. Lohöfer[2]

Containerless materials processing of liquid metals with the use of electromagnetic levitation requires contactless temperature measurement by pyrometry. For high temperatures and under high-vacuum conditions, the vapor pressure of the levitated metal drop increases, leading to evaporation losses of the sample material. This flux condenses on the cold parts of the experimental apparatus including the window in front of the pyrometer. As a result, the intensity of radiation reaching the pyrometer decreases, which is erroneously interpreted as a decrease in temperature. Several methods to protect the pyrometer against contamination have been proposed. In this paper, we report experimental tests of the concepts of shielding windows and mirror optics placed into the optical path between the sample and the pyrometer. Temperature measurements with a periscopic mirror system are also presented.

KEY WORDS: evaporation; high temperature; levitation; liquid metals; microgravity; pyrometry.

1. INTRODUCTION

The containerless electromagnetic levitation technique is one of the most important experimental methods for investigating melting, undercooling, nucleation, and solidification of metallic samples [1]. Additionally, it allows the measurement of thermophysical properties of metals such as surface tension, viscosity, and specific heat even in the undercooled state [2–4]. Containerless processing of liquid samples evokes the demand for a contactless temperature measurement provided by pyrometry.

[1] Paper presented at the Second Workshop on Subsecond Thermophysics, September 20–21, 1990, Torino, Italy.

[2] Institute for Space Simulation, German Aerospace Research Establishment, DLR, D-5000 Köln 90, Germany.

0195-928X/92/0100-0199$06.50/0

The relation between spectral radiance L_b and temperature T is given by Planck's radiation law:

$$L_b(\lambda, T) = \frac{c_1}{\lambda^5} \frac{1}{\exp(c_2/\lambda T) - 1}$$

where c_1 ($1.19 \cdot 10^{-16} \mathrm{W \cdot m^2}$) and c_2 ($0.014388 \mathrm{m \cdot K}$) are the two radiation constants. The above relation is true only for blackbody radiation (emissivity $\varepsilon = 1$). The emissivity of real bodies is defined as

$$\varepsilon(\lambda, T) = \frac{L(\lambda, T)}{L_b(\lambda, T)}$$

The spectral emissivity of any metal is a function of the wavelength and of the temperature. It not only is characteristic for the material but also depends largely on surface conditions such as roughness and oxidation [5]. If the emissivity is nearly constant over a small spectral region, $\varepsilon_1(\lambda_1, T) \approx \varepsilon_2(\lambda_2, T)$, the effect of emissivity can be made negligible by measuring the radiation intensities in two narrow wavelength bands and subsequent evaluating the ratio.

Electromagnetic levitation experiments on earth use inert gas atmosphere as cooling agent. Due to the weak electromagnetic fields necessary in reduced gravity, undercooling even of low melting metals is possible without gas cooling. The ultrahigh vacuum (uhv) conditions provide a considerable improvement of the purity in the leviation chamber and therefore the possibility of higher undercooling. On the other hand, uhv conditions pose a difficult problem for pyrometry, namely, that of contamination of the optical path.

As has turned out during temperature measurements of a levitated liquid metal drop under uhv conditions, even the ratio signal of the pyrometer is not satisfactory. It shows significant deviations from the correct temperatures when contamination arises at the pyrometer window. Furthermore, it reacts sensitively on changes in the spectral emissivity with temperature.

As long as no continuous monitoring of the temperature is required, high-speed pyrometry can be used to circumvent the problem of evaporation and contamination. In undercooling experiments, however, this is not possible. Since nucleation is intrinsically a stochastic process, its onset and the subsequent recalescence of the sample due to the release of the heat of fusion cannot be predicted and continuous temperature measurement is necessary.

Several possibilities for protecting the pyrometer against contamination have been proposed. A set of shielding windows is the most simple

approach in avoiding evaporation effects. When the measurement errors become intolerable, the contaminated window is replaced by a clean one.

An improvement of the shutter concept, which is able to protect the pyrometer only during nonmeasuring periods, is a rotor inserted in the optical path between the sample and the pyrometer. If the dimensions and rotating velocities are suitably chosen, the rotor will be transparent to light but totally absorbing to material flow. Due to the very high rotational speed required, this system is mechanically rather complex, especially for operation in uhv.

An alternative shielding mechanism without moving parts is based on a diffraction grating. By putting a transmission diffraction grating into the optical path normal to the incident radiation of the liquid sample, light will be diffracted but metal atoms will not. Contamination can be avoided by a stop aperture in front of the zero-order maximum [6]. It should be noted that radiated intensity is lost by not using the undiffracted light. Therefore, intensity problems at low temperatures can be expected. Furthermore, constant diffraction spacings and slit widths even in the case of strong evaporation have to be assumed.

Another possibility is a gas jet in front of the pyrometer [7]. The disadvantage of this approach is that the uhv conditions cannot be maintained.

Finally, contamination can be avoided with the help of a mirror [8], where the straight line between the sample and the pyrometer is blocked. A subsequent development is a periscopic mirror system, which has been presented in the literature [9].

We were confronted with this contamination problem in the course of experiments in TEMPUS [10], an electromagnetic leviation facility designed to operate in microgravity. A schematic view of TEMPUS is given in Fig. 1. The central part of the module is a cylindrical stainless-steel vacuum chamber. The heating and positioning coils fixed in the center of the cylindrical chamber are connected to semiconductor generators.

The TEMPUS laboratory module is equipped with a two-color pyrometer with a sampling rate of 1 MHz. It works in the infrared region, covering a temperature range from 300 to 2400°C. The first temperature signal refers to the wavelength range between 1 and 2.5 μm, whereas the second signal refers to 3–4 μm. From these two signals the ratio temperature is calculated.

To overcome the contamination problems concerning the TEMPUS project, the concept of a double mirror system seems to be promising [11]. It is placed in front of the pyrometer window, blocking the direct optical path between the sample and the pyrometer optics. Assuming a collisionless ballistic trajectory of the atoms, the evaporated particles will

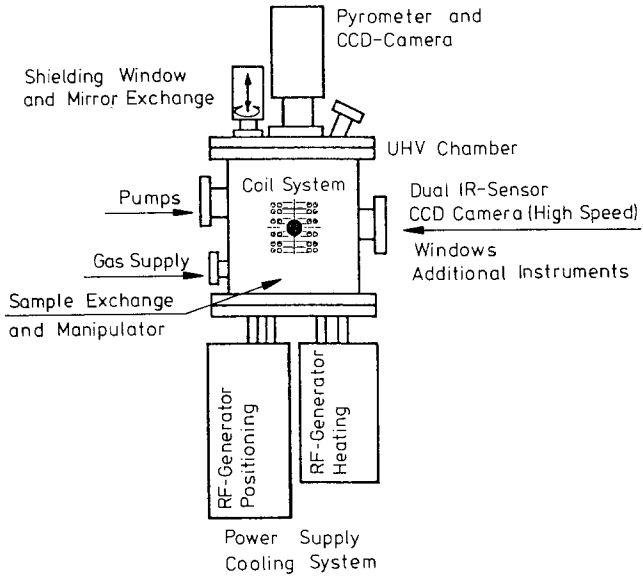

Fig. 1. Schematic design of the TEMPUS facility.

condense onto that mirror surface facing the sample. Reliable temperature measurements with the double mirror optics are assured as long as the optical quality of the mirror is not influenced severely.

In a series of preliminary experiments, we first tested the contamination behavior of shielding windows. Subsequently, we investigated the behavior of single mirrors on glassy and metallic substrates. Finally, a double mirror system was used. These tests were performed under realistic experimental conditions, using hot and liquid metallic samples. The optical quality of the mirror surfaces was verified by temperature measurement of a blackbody radiator.

2. SHIELDING WINDOWS

To illustrate the problems of correct temperature measurements when levitating a liquid metal drop under uhv conditions the temperature–time profile presented in Fig. 2 is considered. The profile was recorded with a two-color pyrometer while heating an Al sample in the TEMPUS laboratory module using CaF_2 shielding windows. As long as the vapor pressure is low enough, pyrometry is not critical. Difficulties arise in approaching and surpassing the melting temperature under ultrahigh vacuum. First, the temperature profile makes evident the change of ε with

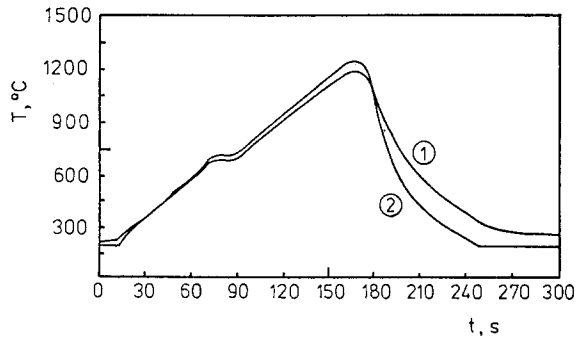

Fig. 2. Temperature–time diagram of Al using a CaF_2 shielding window showing (1) short (1- to 2.5-μm)- and (2) long (3- to 4-μm)-wavelength signal.

temperature for the different wavelength regimes. Up to the melting point, both pyrometer signals yield the same temperature. At higher temperatures there are deviations which become larger. Second, the vapor pressure and the evaporation losses of the sample material strongly increase in the liquid phase, leading to a contamination of the CaF_2 windows. In the case of Al with a relatively low vapor pressure caused by the stable oxide surface layer, condensation effects become significant at temperatures above $T = 1000°C$. After the Al oxide is removed from the sample surface, the evaporating particles condense on the shielding window. The radiation intensity reaching the pyrometer detectors decreases, leading to an apparent decrease in the sample temperature. This is even more pronounced for the temperature signal 2 referring to the longer wavelength range. Thus, even the ratio signal of the pyrometer is not reliable. The temperature would change remarkably if the contaminated window was replaced by a new fresh one. Therefore, shielding windows do not seem to solve the problem of reproducible and correct temperature data. Furthermore, for multiuser facilities such as TEMPUS with a large number of experiments during a space flight, the shielding of windows becomes a critical problem.

3. MIRROR SYSTEMS

The basic idea was to use a periscopic mirror system instead of shielding windows. The emissivity and reflectivity behavior of a mirror is characteristic for the material as well as dependent on its surface structure and appearance. For certain parameters, especially the vapor pressure, vacuum, and adhesive properties, the evaporated sample material will not severely influence the optical quality of the mirror surface, consisting of the

same material. Furthermore, one can expect that the absorption and reflection behavior of the metallic mirror surface remains unchanged during the condensation of sample material.

3.1. Production of Metallic Mirror Surfaces

Metal mirrors of Ni and Al on glassy substrates were made in a test facility similar to the TEMPUS module. Figure 3 shows the schematic design of the experimental unit. The glass substrate, in this case comparable to a shielding window, is exposed to the evaporation of a hot sample under a pressure of about 10^{-6} HPa. It is positioned in front of the pyrometer optics inside the vacuum chamber blocking the straight line between the sample and the pyrometer. In Fig. 4, a typical temperature–time diagram of Ni is represented. Temperature was measured with a single-channel pyrometer with a wavelength range from 0.8 to 1.1 μm and a temperature range from 800 to 2300°C. The condensation

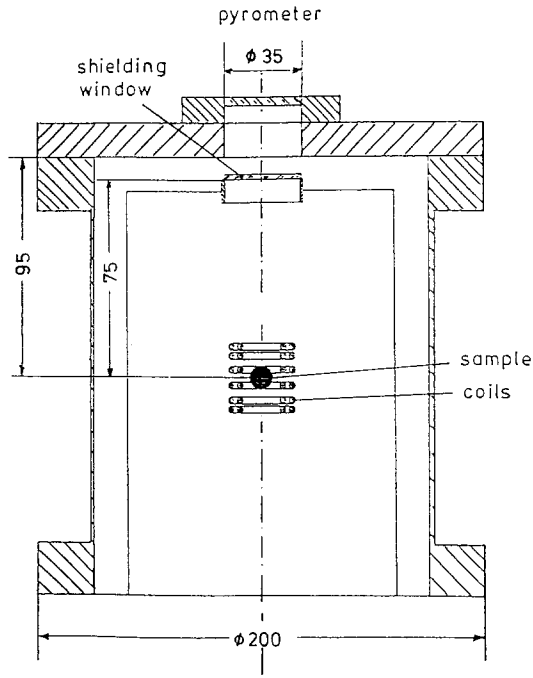

Fig. 3. Schematic design of the TEMPUS test facility (mirror substrate) [by courtesy of Dornier, Technical Note 2069-3107 DS/01 (5/89)].

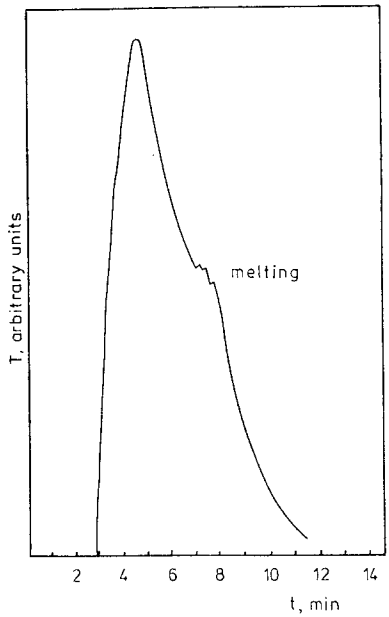

Fig. 4. The apparent temperature as a function of time, showing a strong decrease due to evaporation onto the shielding window. At $t = 5$ min the melting point during heating is reached.

onto the substrate could be observed by means of the radiation intensity decrease even when the Ni sample is solid. During heating the Ni sample with a constant heating power, the temperature signal shows a strong decrease due to the evaporation onto the glassy substrate acting like a shielding window. Whereas the true temperature is rising to approximately 150°C above the melting point, the apparent temperature calculated from the pyrometer signal decreases. This can be seen from the fact that the melting of the sample, evident by a plateau in the pyrometer signal, occurs

Table I. Reflectivity of Al and Ni Mirrors as a Function of Wavelength

Material	ρ_1, 0.8–1.1 μm	ρ_2, 1.0–2.5 μm	ρ_3, 3.0–4.0 μm
Nickel	0.70–0.72	0.83–0.84	0.89–0.90
Aluminum	0.88	0.91–0.93	0.93–0.95

at the decreasing flank of the profile. Already after 8 min, the glass substrate became opaque due to the condensed material. It took about 15 min to reach a satisfactory mirror surface.

The optical quality and the reflectivity of the metal mirror were checked by measuring the temperature of a blackbody which was mounted on an optical bench at a right angle to the pyrometer. The mirror was fixed at a suitable distance with an angle of 45° to the blackbody and the pyrometer optics. As a result the deviations in the temperature assuming a constant emissivity $\varepsilon = 1$ with and without the mirror were measured. This temperature difference can be expressed as a decrease in the emissivity of the blackbody from $\varepsilon = 1$ to some lower values. The reflectivity of the metal mirrors corresponds to the emissivity necessary to compensate this difference. Table I summarizes the results concerning the reduced emissivity when using Al or Ni mirrors to measure the temperature of blackbody radiation. The average emissivities determined with two pyrometers in three wavelength ranges are listed for Ni and Al mirror surfaces.

3.2. Evaporation Experiments with the Double Mirror System

Electromagnetic levitation experiments using the double mirror against contamination effects were also performed in the TEMPUS test facility. The mirror was fixed at the upper flange of the vacuum chamber (Fig. 5). During the first experiment, a Ni mirror was facing the liquid sample, whereas an Al mirror was mounted facing the pyrometer. The Ni–Al arrangement was chosen because Ni was going to be processed and thus the evaporated Ni particles condense onto the Ni mirror surface. The Al mirror has the advantage of a relatively high reflectivity compared to Ni and will not be coated with Ni vapour. The Ni sample was heated with a constant heating power to about 1570°C. The experiment lasted 18 min, of which the sample was liquid for 15 min. During this time, the temperature was nearly constant, as is visible in the temperature–time diagram (Fig. 6). A similar measurement was performed later using the same Ni–Al double mirror. A Ni sample was melted and solidified seven times to investigate whether the maximum temperature is reproducible. The final temperatures agreed within 10°C (Fig. 7). For this reason, the reflectivity of the double mirror seems to be constant during the entire experiment. This experiment was repeated with a Ni–Al mirror exposed to a liquid Al sample at 1100°C. The temperature signal of the pyrometer was almost constant for 17 min. Compared to the experiments using CaF_2 shielding windows, where a temperature measurement of liquid Al was impossible after 6 min, the double mirror is a major improvement.

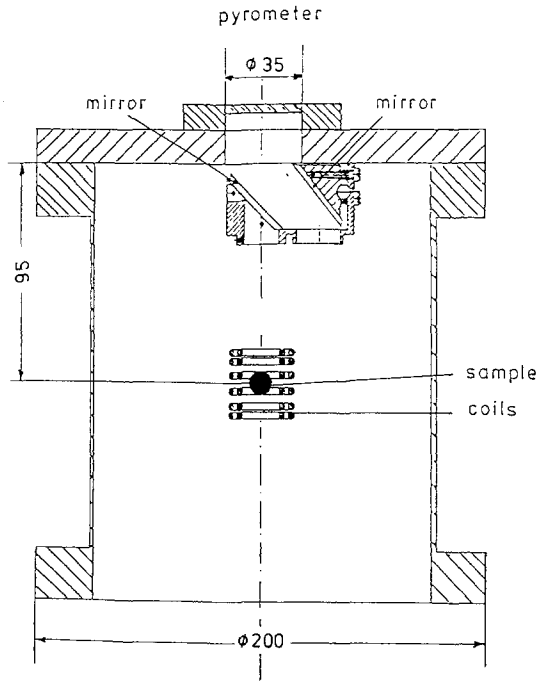

Fig. 5. Schematic design of the TEMPUS test facility (double mirror) [by courtesy of Dornier, Technical Note 2069-3107 DS/01 (5/89)].

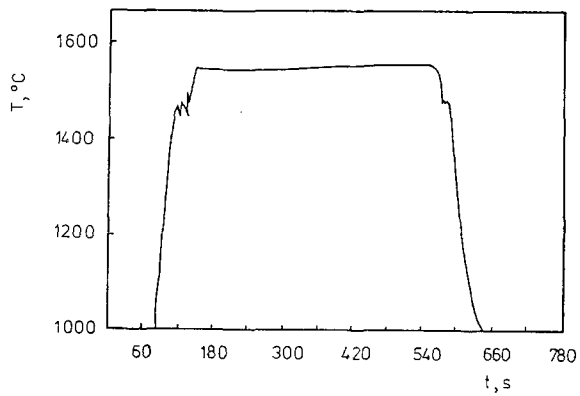

Fig. 6. Temperature–time diagram of Ni using a Ni–Al double mirror showing constant temperature over 10 min.

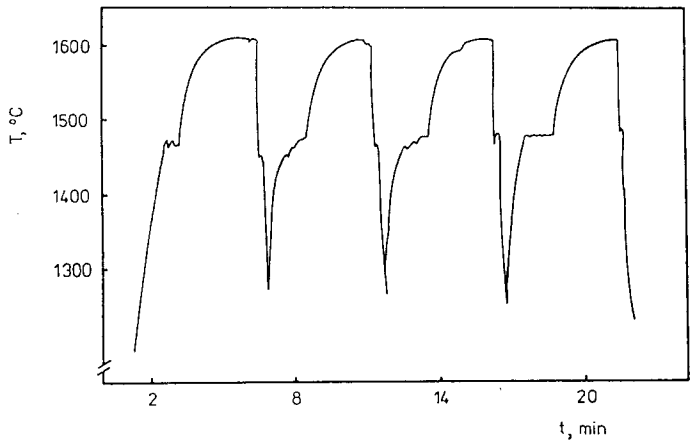

Fig. 7. Temperature–time diagram of Ni using a Ni–Al double mirror showing repeated heating cycles and reproducible maximum temperatures.

3.3. Reflectivity of Double Mirror Systems

Before the double mirror system was integrated into the TEMPUS test facility, the total reflectivity of the mirror was measured. The pyrometer, the double mirror, and the blackbody radiator were mounted on an optical bench in such a way that the path of rays fits to the geometric configuration. The measurements of the radiation attenuation caused by the periscope lead to the emissivity data for the pyrometer or reflectivities of the mirror systems, respectively.

As verification, the reflectivity of the periscopic mirror system was compared with the reflectivities of the single metal mirrors. The products of

Table II. Reflectivity of Ni–Al Double Mirrors (in the Wavelength Range 0.8–1.1 μm) Before and After Contamination with Ni and Al

Material	ρ_1
Single mirrors $\rho_1(\text{Al}) \times \rho_1(\text{Ni})$	0.63
Double mirror Ni–Al, clean	0.67
Double mirror Ni–Al with Ni, run No. 1	0.61
Double mirror Ni–Al with Ni, run No. 2	0.62
Single mirrors $\rho_1(\text{Al}) \times \rho_1(\text{Al})$	0.77
Double mirror Ni–Al with Al, run No. 1	0.76

$\rho(\text{Al}) \times \rho(\text{Ni})$ and $\rho(\text{Al}) \times \rho(\text{Al})$ are consistent with the reflectivities of the double mirrors within the error margins of 5%.

After the first evaporation experiment with a Ni sample, the reflectivity of the Ni–Al mirror system decreased by approximately 10% (Table II). After the second experiment run, however, the reflectivity of the Ni–Al mirror coincided with the value after the first run within 1%. Comparing the data of the Ni–Al basic mirror and the values after it had been exposed to a liquid Al sample and had been coated with Al, the reflectivity increased by about 15%. This result meets the expectation because the Al mirror surface showed a better reflectivity than the Ni surfaces (Table I).

4. SUMMARY

The application of a periscopic mirror system seems to be a possibility for solving the difficulties of temperature measurement under ultrahigh-vacuum conditions. First experiments lead to the results that the optical quality of the double mirror does not change very drastically during the evaporation process. But this is true only if mirror material and condensing material are identical. Otherwise one has to wait until the evaporated particles have formed a dense layer on the basic mirror, thereby creating its own mirror surface. During the experiments there are, to a certain extent, no alterations in the reflectivity behavior observable. Further investigations are necessary and desirable with other metals to get more information, especially about the mechanical stability and characteristic properties of suitable mirror systems.

ACKNOWLEDGMENTS

Thanks are due to Dornier GmbH, Dept. RGMM, for placing the TEMPUS test module at disposal. We also thank J. Piller for scientific and experimental support.

REFERENCES

1. R. Willnecker, D. M. Herlach, and B. Feuerbacher, *Appl. Phys. Lett.* **49**:1339 (1986).
2. B. J. Keene, K. C. Mills, A. Kasama, and A. McLean, *Metallurg. Transact.* **B17**:159 (1986).
3. J. Schade, A. McLean, and W. A. Miller, in *Undercooled Alloy Phases*, Proc. 115th Annu. Meet. TMS-AIME, E. W. Collins and C. C. Koch, eds. (1986), p. 233.
4. I. Egry, B. Feuerbacher, G. Lohöfer, and P. Neuhaus, *ESA* **SP-295**:257 (1990).
5. Y. S. Touloukian and D. P. De Witt, *Thermophysical Properties of Matter, Vol. 7, Thermal Radiative Properties—Metallic Elements and Alloys* (Plenum Press, New York, 1972).
6. D. Neuhaus, German Patent P4008327, *Rev. Sci. Instr.* **62**, Vol. 9 (1991).

7. M. J. Smeljanskij, *Elektrotermija* **39**:18 (1964).
8. M. V. Gartman, V. G. Glebovskij, and A. N. Izotov, *Dokla Simpozijuma 124* (Nauka, Moscow, 1971).
9. A. J. Spring Thorpe, T. P. Humphreys, A. Majeed, and W. T. Moore, *Appl. Phys. Lett.* **55**:2138 (1989).
10. J. Piller, R. Knauf, P. Preu, G. Lohöfer, and D. M. Herlach, *ESA* **SP-265**:437 (1987).
11. P. Neuhaus, DLR, Internal Report, IB 9 (1990).

Printed in Belgium